Effect of Stoichiometry on Liquid Crystalline Supramolecular Polymers Formed with Complementary Nucleobase Pair Interactions

KELLY A. BURKE, SONA SIVAKOVA, BLAYNE M. McKENZIE, PATRICK T. MATHER, STUART J. ROWAN

Department of Macromolecular Science and Engineering, Case Western Reserve University, Cleveland, Ohio 44106-7202

Received 11 January 2006; accepted 12 February 2006
DOI: 10.1002/pola.21626
Published online in Wiley InterScience (www.interscience.wiley.com).

ABSTRACT: We report herein studies on the liquid crystalline behavior of a series of supramolecular materials that contain different ratios of two complementary symmetrically-substituted alkoxy-bis(phenylethynyl)benzene AA- and BB-type monomers. One monomer has thymine units placed at either end of the rigid mesogenic core, while the other has N^6-(4-methoxybenzoyl)-adenine units placed on the ends. Differential scanning calorimetric and polarized optical microscopy studies have been carried out on these systems. These studies show that the material's behavior is strongly dependent on its thermal history. As a result, the materials can exhibit, on heating, either a liquid crystalline phase, a crystalline phase, or the coexistence of crystalline and liquid crystalline regions. © 2006 Wiley Periodicals, Inc. J Polym Sci Part A: Polym Chem 44: 5049–5059, 2006

Keywords: liquid crystalline polymers; molecular recognition; self-assembly; supramolecular structures

INTRODUCTION

The ability to use noncovalent interactions to assemble monomeric units into polymeric aggregates, supramolecular polymerization,[1] opens the door to materials that potentially exhibit a new matrix of properties. One major advantage of such a self-assembly process is the ability to control the resulting supramolecular nanostructure of the polymer aggregates by tailoring the structure of the monomer.[2,3] Another aspect that differentiates supramolecular polymers from more conventional covalently bonded structures is their dynamic nature, which has potentially significant consequences for the thermomechanical properties of such systems. The backbones of the resulting polymeric systems contain noncovalent bonds, in addition to covalent bonds, which imparts reversibility and temperature sensitivity upon the system. The properties of such noncovalently bound aggregates have a strong dependence not only on their core components, but also on the nature (stability and dynamics) of the supramolecular interactions, which control the self-assembly process. The degree of polymerization (DP) of the aggregate depends, to a large extent, on the strength of the supramolecular interaction between the monomers, as well as the monomer concentration. This has led to the development of a range of supramolecular motifs that exhibit large binding constants ($>10^6$ M^{-1}). In particular, motifs that rely on either hydrogen bonding[4–6] or metal/ligand interactions[7] have been designed and utilized successfully in the preparation of supramolecular materials.[8–16]

Correspondence to: S. J. Rowan (E-mail: stuart.rowan@case.edu) or P.T. Mather (E-mail: patrick.mather@case.edu)

Journal of Polymer Science: Part A: Polymer Chemistry, Vol. 44, 5049–5059 (2006)

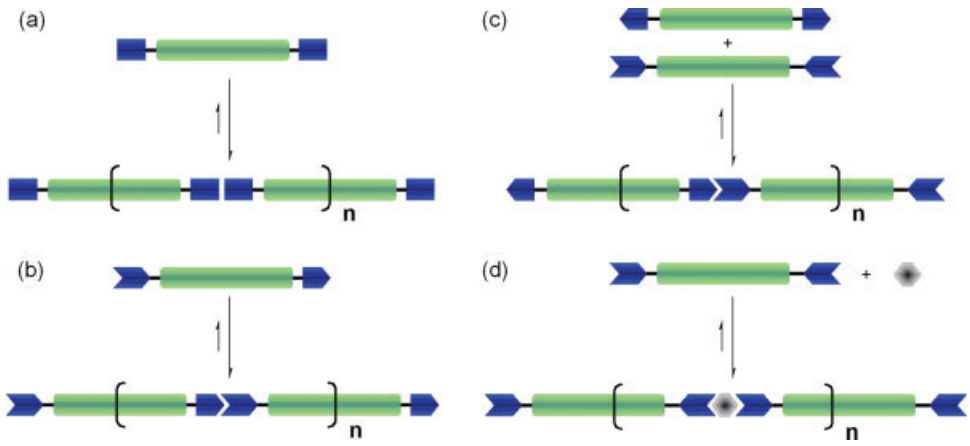

Figure 1. Schematic representation of the self-assembly polymerization of (a) a homoditopic monomer with self-associating chain ends to yield a $(A)_n$ polymer, (b) a heteroditopic monomer with complementary chain ends to yield a $(AB)_n$ supramolecular polymer, (c) two complementary homoditopic monomers to yield a $(AA\text{-}BB)_n$ supramolecular polymer, and (d) a metallo-supramolecular polymer. [Color figure can be viewed in the online issue, which is available at www.interscience.wiley.com.]

The dynamic nature of the polymerization/depolymerization process confers unusual mechanical properties on such materials. Anything that affects either the degree of interaction between the binding motifs and/or the monomer concentration will drastically alter the DP of the material, and consequently, the properties of these "dynamic" polymers should be very sensitive to environmental conditions. Thus, the development of materials self-assembled through a supramolecular polymerization process opens the door to systems that are extremely thermally responsive and would exhibit low melt viscosities for easy processing and/or recycling.

There are a number of ways in which supramolecular polymerizations can be achieved, but conceptually, the simplest way is to attach supramolecular motifs to the ends of a core unit (Fig. 1). Depending on the nature of the self-assembling motif, there are a number of classes of supramolecular polymerizations that can be envisaged, each with their own advantages and disadvantages. The simplest class of a main-chain supramolecular polymer is one that has self-complementary units attached to either end of the core and thus results in a self-assembling $(A)_n$ polymer [Fig. 1(a)]. If the supramolecular motif used in the assembly of the polymer is asymmetric (i.e., consists of two different complementary units), then the supramolecular polymer will be formed only when both of these complementary units are present. A heteroditopic monomer, in which both complementary units are placed on the same molecule, results in a self-assembling $(A\text{-}B)_n$ polymer [Fig. 1(b)]. However, homoditopic monomers, which have one of the complementary units placed on both ends of the core (e.g., A-A or B-B), will only exhibit polymer-like properties upon mixing the two complementary monomers [e.g. Fig. 1(c)]. A subset of this class of supramolecular polymer is metallo-supramolecular polymers, in which monomers have ligands attached to either end and polymerize upon the addition of a metal ion [Fig. 1(d)]. In these last two cases, there exists the potential that the formation of the supramolecular polymer will result in the expression of new functional and/or mechanical properties, which are not exhibited by the individual monomers.

As part of a program aimed at investigating new supramolecular materials, we have focused our attention on two distinct classes of supramolecular motifs. The first type of motif we have been investigating is metal-ligand interactions, in which the thermodynamic driving force for polymerization is the large degree of interaction between the metal ion and the ligand.[11] Another class of supramolecular motifs that we have utilized to make supramolecular polymers are the nucleobases. In this case, on account of the relatively weak interaction between single nucleobases, we have focused on the use of additional organizing effects to enhance the degree of interactions between the monomers.[17,18] One method-

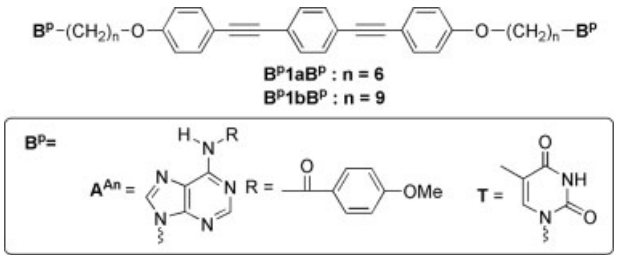

Figure 2. Chemical structures of the homoditopic (A-A, B-B) nucleobase end functionalized bis(phenylethynyl)benzene monomers ($\mathbf{B^P1aB^P}$ and $\mathbf{B^P1bB^P}$). $\mathbf{B^P}$, nucleobase derivative.

ology that has been utilized to enhance the interaction between molecules is the ordering effects of liquid crystallinity that lead to liquid crystalline supramolecular polymers[19–22] with relatively weak hydrogen-bonding interactions between monomers.[23,24]

Recently, we have reported the investigation of homoditopic monomers (Fig. 2) in which the nucleobase thymine (**T**) and the nucleobase derivative N^6-(4-methoxybenzoyl)-adenine ($\mathbf{A^{An}}$) are substituted on both ends of an alkoxy-substituted bis(phenylethynyl)benzene core ($\mathbf{B^P1aB^P}$ and $\mathbf{B^P1bB^P}$).[18] We have shown that the binding motif which consists of thymine and N^6-(4-methoxybenzoyl)-adenine can be used to control the aggregation of symmetrically-substituted alkoxy-bis(phenylethynyl)benzene units resulting in A-A/B-B type polymeric species, which form relatively stable LC phases. Concurrent with the formation of the viscous birefringent phases, the materials also demonstrate the ability to form oriented, fluorescent fibers. Thus, we have utilized the functionality of the core unit, to aid LC formation and impart fluorescent behavior, in conjunction with the self-assembly capability of the nucleobases, which not only aids LC formation but also imparts polymer-like properties to the material; i.e., fiber formation. In our previous article, liquid crystallinity of a 1:1 blend of $\mathbf{A^{An}1aA^{An}}$**:T1bT** was reported, with multiple LC transitions appearing between the lowest temperature endotherm at 120 °C and an isotropization temperature of 178 °C. Furthermore, WAXD analysis confirmed the lowest temperature mesophase is smectic-C, consistent with POM observations at 125 °C showing a granular birefringent texture. Addition of a monofunctional dodecyl-$\mathbf{A^{An}}$ to a similar 1:1 blend of $\mathbf{A^{An}1aA^{An}}$**:T1aT** (6 carbon spacer in the **T** compound) resulted in dramatic destabilization of liquid crystallinity, likely due to a decrease in supramolecular polymerization degree. In contrast, and surprisingly, a 1.5:1 (off-stoichiometric) mixture of **T1bT** with $\mathbf{A^{An}1bA^{An}}$ did not feature significantly different phase behavior when compared with the 1:1 blend, although fibers could not be formed from the melt, indicating low molecular weight. We herein report investigations into several mixtures of $\mathbf{A^{An}1aA^{An}}$ with **T1bT**; specifically, 1.5:1, 1:1, and 1:1.5, focusing specifically on phase behavior ascertained with calorimetry and light microscopy and revealing that only the 1:1 mixture exhibits rich mesomorphism with multiple transitions.

EXPERIMENTAL

Materials

$\mathbf{A^{An}1aA^{An}}$ with **T1bT** and were prepared according to literature procedures.[18] The mixed samples were prepared by dissolving the monomers in dichloromethane/methanol solutions and adding the appropriate amount of the two solutions together, followed by removal of the solvent and drying in a vacuum oven at 40 °C overnight.

Differential Scanning Calorimetry

Differential Scanning Calorimetry (DSC) experiments were performed on a TA Instruments Q100 apparatus in a flowing N_2 atmosphere. Unless otherwise stated, the samples were first equilibrated at −90 °C, heated at 20 °C/min to 200 °C and held at that temperature for 1 min, cooled to −90 °C at 20 °C/min and held for one minute, and finally heated at 20 °C/min to 200 °C. Two additional experiments, with different thermal histories, on the 1:1 $\mathbf{A^{An}1aA^{An}}$**:T1bT** blend were conducted: one in which the sample was heated to 230 °C and the other in which the sample was annealed. For the experiment up to 230 °C, the sample was first equilibrated at −90 °C, heated at 20 °C/min to 230 °C and held 1 min, cooled to −90 °C at 20 °C/min, and held for 1 min, heated at 20 °C/min to 230 °C, and finally cooled to −90 °C at 20 °C/min. For the annealing experiment, the sample was again equilibrated at −90 °C, heated at 20 °C/min to 200 °C, and held for 1 min before being cooled to −90 °C at 20 °C/min. For the second heat, the sample was heated to 160 °C at 20 °/min, where it was held for 30 min before being cooled to −90 °C. The sample was then heated according to the same procedure as the

first heat. This relatively high heating/cooling rate was employed to afford sensitivity even for small samples. Samples weighing from 3 to 4 mg were encapsulated in aluminum pans for testing. Temperatures corresponding to minima of the DSC endothermic peaks of the second heating traces were assigned as transition temperatures. The glass transition temperature, T_g, was determined from the midpoint of the heat flow stepwise decrease in the second heating trace.

Polarizing Optical Microscopy

Polarizing optical microscopy (POM) studies were performed using an Olympus BX51 microscope equipped with crossed polarizers, a HCS402 hot stage (Instec Inc.) and a digital camera (14.2 Color Mosaic Model from Diagnostic Instruments, Inc.). Images were acquired from the camera at selected temperatures using Spot software (Diagnostic Instruments, Inc.). Spatial dimensions were calibrated using a stage micrometer with 10 μm line spacing. A 20×/0.4 NA achromat long working-distance objective lens (Olympus LMPlanFI) was employed. The samples used for POM analysis were sandwiched between two glass coverslips and melted at 180 °C, with care being taken to avoid coverslip flexure that would lead to void formation, and quenched to room temperature. The Instec hotstage was equipped with a liquid nitrogen LN_2-P cooling accessory for accurate temperature control during heating and cooling runs. The thermal history of the samples included first heating to 200 °C at 10 °C/min (clearing or melting the samples), holding for 1 min, cooling to −25 °C at 10 °C/min, and finally holding at this temperature for 2 min. The samples were then heated to 200 °C at 10 °C/min, held at 200 °C for 1 min, and cooled to −25 °C at 10 °C/min. Optical micrographs were collected during these second heating and cooling steps.

RESULTS AND DISCUSSION

Thermal Studies of Different Ratios of $A^{An}1aA^{An}$:T1bT

DSC studies were conducted on the blends to reveal the dependence of phase behavior on blend stoichiometry. Figure 3 shows the DSC first cooling and second heating traces of the 1:1, 1:1.5, and the 1.5:1 **$A^{An}1aA^{An}$:T1bT** blends, with heating and cooling traces paired by material and the cooling trace always appearing above the heating trace. In the first cooling and second heating runs of the 1:1 blend, curves c and d of Figure 3, respectively, a T_g of was observed to be ~74 °C. The existence of a definitive T_g is consistent with the lack of crystallization (prior to the occurrence of T_g) for these two traces and reveals that the blend is a type of glassy liquid crystal. This material also has several endothermic peaks, on heating, between 90 and 150 °C, which correspond to the LC phase transitions observed in the POM study of this material. From our prior work,[18] we know that the lowest temperature phase (above T_g) is smectic-C; however, the additional 2–3 phases existing at higher temperature (seen most readily on cooling) up to the clearing (isotropization) temperature are unknown. Unlike our prior work, which featured heating to 220 °C and used a lower heating rate of 5 °C/min during first-heating, we observe here a large exothermic peak centered at 159 °C, presumably due to recrystallization of a high-T_m crystal, followed by an associated endothermic transition at 185 °C. As we will discuss later, the exothermic transition is accompanied by textural

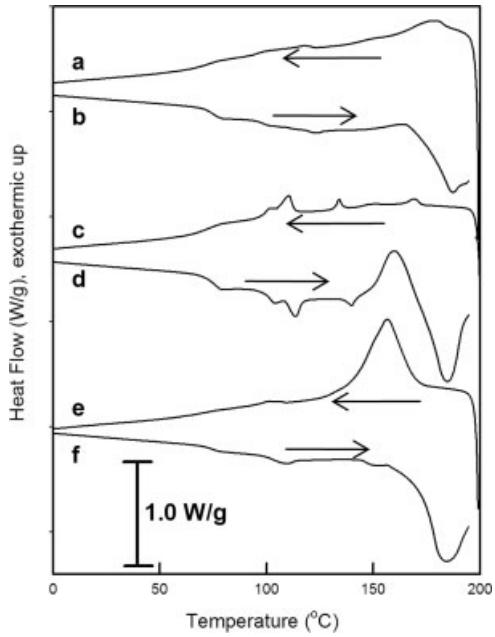

Figure 3. DSC first cooling and second heating traces of the **$A^{An}1aA^{An}$:T1bT** 1:1.5, 1:1, and 1.5:1 blends. The cooling curves correspond to the following blend ratios of **$A^{An}1aA^{An}$:T1bT**: (a) 1:1.5, (c) 1:1, and (e) 1.5:1. The heating curves are the blend ratios: (b) 1:1.5, (d) 1:1, and (f) 1.5:1.

brightening and coarsening when observed with polarizing optical microscopy. The ensuing large endothermic transition is interpreted as a conventional melting point. The first cooling curve of this blend (Fig. 3, curve c) shows four exothermic transitions between 175 and 90 °C, marking first-order phase transitions: I → LC_1→ LC_2 → LC_3 → SmC. The temperatures and latent heats for each transition are as follows: 169.5 °C (0.827 J/g), 134.1 °C (0.774 J/g), 110.5 °C (1.85 J/g), and 101.3 °C (0.249 J/g), respectively. During this first cooling run, no large crystallization exotherm was observed. We return to a discussion of this 1:1 blend in more detail below, but first let us discuss the phase behavior of nonstoichiometric blends as observed also with DSC.

Adding a 50% molar excess of **T1bT** to the blend did not alter T_g, but significantly decreased the sharpness of endothermic and exothermic transitions on heating and cooling, respectively. In particular, the second heating trace of the 1:1.5 **A^{An}1aA^{An}:T1bT** blend (Fig. 3, curve a) shows a T_g of ~74 °C, which is similar to the 1:1 blend and indicates that excess **T1bT** does not affect T_g despite an expectation of a lower degree of polymerization of the supramolecular species. In this blend, the endotherms between 90 and 150 °C are clearly much smaller than in the 1:1 blend, blending into one broad transition peaked at 123 °C. The exotherms between 65 and 190 °C in the first cooling trace (Fig. 3, curve a) are also smaller than in the 1:1 blend. These differences are reflected in the POM study of this material, which will be discussed below. Similar to the 1:1 blend, however, is the appearance of a large exotherm/endotherm sequence on heating, indicating recrystallization and melting.

Adding 50% molar excess of **A^{An}1aA^{An}** to the blend (1.5:1 **A^{An}1aA^{An}:T1bT** blend) is more disruptive to liquid crystalline phase formation than the case of added **T1bT**, as we find facile crystallization on cooling (identifiable by a large latent heat) and near-elimination of additional cooling exotherms that would represent LC phase formation. The first cooling trace for this blend (curve e), having previously melted the sample through heating to 200 °C, shows a large crystallization exotherm centered at 156.5 °C. Subsequent heating of this sample (curve f) reveals a T_g at ~74 °C, clearly unaffected by the component in excess when compared with curve d of the same figure. At 107.3 °C there is a small endotherm that does not cause any noticeable changes in the POM images, while a large melting endotherm at 185 °C is apparent. Interestingly, this is precisely the same melting temperature as was observed for the heating-crystallized 1:1 blend.

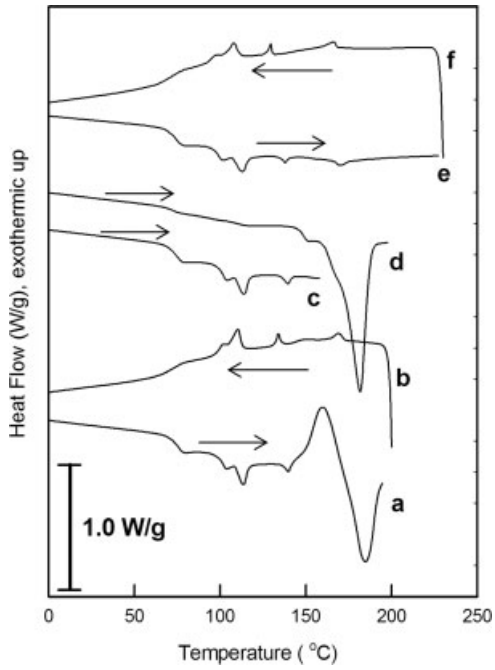

Figure 4. DSC traces of the 1:1 **A^{An}1aA^{An}:T1bT** blend. Curves (a) and (b) represent second heating and cooling traces, respectively, at 20 °C/min. Curve (c) represents a second heating run stopped at 160 °C to anneal for 30 min, yielding the third heating trace, curve (d). Curves (e) and (f) are the second heating and cooling traces for a sample heated to 230 °C.

Given the propensity of the 1:1 blend to crystallize upon heating, but not on cooling (Fig. 4, curves a, b, which are reproduced from Fig. 3 for direct comparison), coupled with the obscuring of minor transitions on cooling of the 1.5:1 **A^{An}1aA^{An}:T1bT** blend due to facile crystallizing, we designed and executed additional DSC experiments for the 1:1 blend (Figure 4). First, we interrupted the second heating of this blend to anneal at 160 °C for 30 min, allowing complete crystallization, then cooled to $T = -90$ °C (−20 °C/min) and heated again to 200 °C (20 °C/min). Accordingly, Figure 4 (curves c, d) shows the second and third heating, respectively, of the **A^{An}1aA^{An}:T1bT** 1:1 blend that follow this thermal history. The second heat (Fig. 4, curve c), programmed to stop at 160 °C, showed a T_g at 73.2 °C followed by three endotherms centered at 103.3, 114.0, and 139.7 °C. After crystallizing the sample

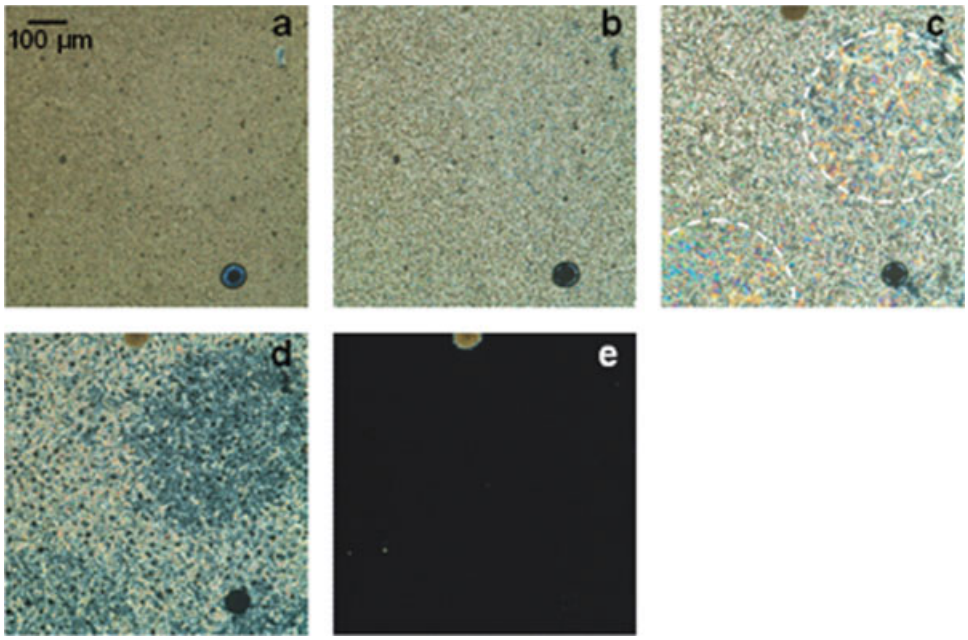

Figure 5. POM images under crossed polarizers of the **$A^{An}1aA^{An}$:T1bT** 1:1 blend. These micrographs were acquired on the second heat at (a) 112.3 °C, (b) 148.4 °C, (c) 166.3 °C, (d) 173.3 °C, (e) 177.8 °C. [Color figure can be viewed in the online issue, which is available at www.interscience.wiley.com.]

at 160 °C for 30 min and cooling to −90 °C at 20 °C/min, the third heat (Fig. 4, curve d) shows a similar T_g again at 71.3 °C; however, the smaller endothermic transitions witnessed during the prior heating disappeared and the melting endotherm at 181.7 °C became larger and much more defined. Ostensibly, crystallization of the high-melting (∼185 °C) crystal eliminates liquid crystalline phase formation in these blends, whether stoichiometric or off-stoichiometric, indicating that the crystalline phase is preferred, energetically, but kinetically avoidable. In this manner, the materials are monotropic, rather than enantiotropic in their phase behavior.

To further understand the propensity of this blend to crystallize, our second additional DSC experiment involved heating to 230 °C, rather than 200 °C, hypothesizing incomplete melting of crystals in the latter case which resulted in residual crystallization nuclei and thus facile crystallization. Figure 4, curves e and f, show the second heating and second cooling traces following prior heating to 230 °C. Indeed, no evidence of recrystallization or melting is observed, consistent with our hypothesis.

POM of Different Ratios of $A^{An}1aA^{An}$:T1bT

Polarizing optical microscopy (POM) was used to examine the microstructure of the blends following a similar heating protocol as described above for DSC measurements, except using a lower heating/cooling rate of 10 °C/min due to instrument limitations. Although inadequate to allow LC phase identification, our observations were helpful in corroborating interpretations of DSC results discussed earlier. The POM images of the 1:1 blend of **$A^{An}1aA^{An}$:T1bT** (Fig. 5) show liquid crystallinity (birefringence and fluidity) for temperatures above T_g. Figure 5(a) shows a POM image at 112.3 °C. This low-temperature LC phase transitions to a different liquid crystalline phase, recorded at 148.4 °C, visible as a clear and sharp brightness change [Fig. 5(a,b)]. Continued heating of the 1:1 blend causes the blend to crystallize, as discussed earlier, and reveal radially growing bright and coarse structures [Fig. 5(c), white dashed areas]. This interpretation is confirmed by the presence of an exotherm at 159 °C in the DSC traces [Fig. 3(d)]. Around 173 °C the recrystallized material starts to melt and become isotropic [Fig. 5(d)]. The surrounding LC material later clears (loses birefringence) to give a fully isotropic phase at 177 °C [Fig. 5(e)].

During heating of the 1:1.5 **$A^{An}1aA^{An}$:T1bT** blend (excess **T**), no LC transitions are apparent, but a brightening and coarsening occurs at

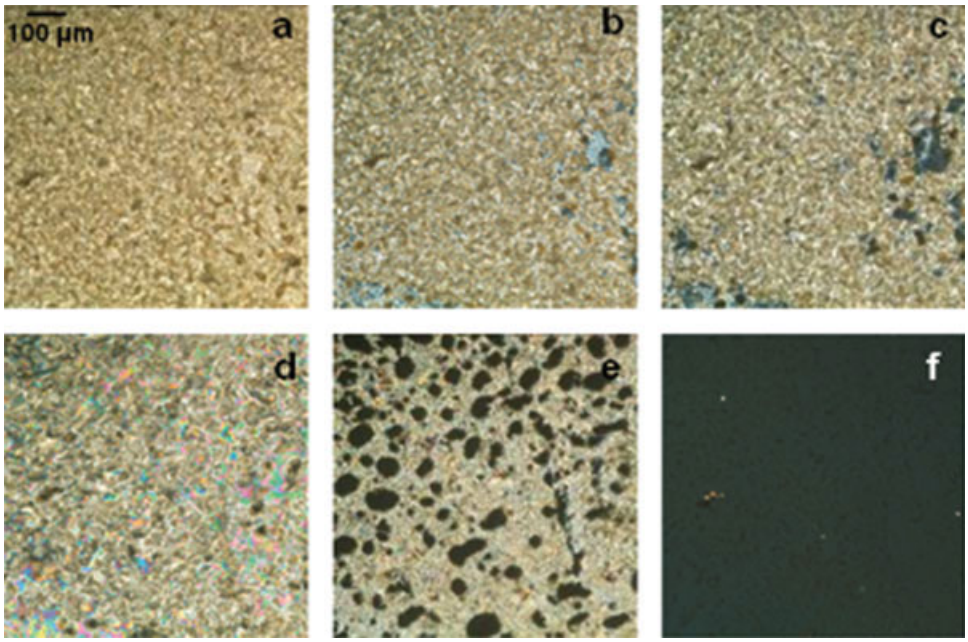

Figure 6. POM images under crossed polarizers of the $\mathbf{A^{An}1aA^{An}}$**:T1bT** 1:1.5 blend. These micrographs were acquired on the second heat at (a) 95.2 °C, (b) 161.7 °C, (c) 175.0 °C, (d) 179.6 °C, (e) 185.8 °C, (f) 200.9 °C. [Color figure can be viewed in the online issue, which is available at www.interscience.wiley.com.]

temperatures corresponding to the crystallization exotherm witnessed in Figure 3(b) (Fig. 6). The material completely melts by 200 °C [Fig. 6(f)]. In contrast to the **T1bT**-excess blend, but similar to the 1:1 blend, hot-stage microscopy of the 1.5:1 blend of $\mathbf{A^{An}1aA^{An}}$**:T1bT** revealed two

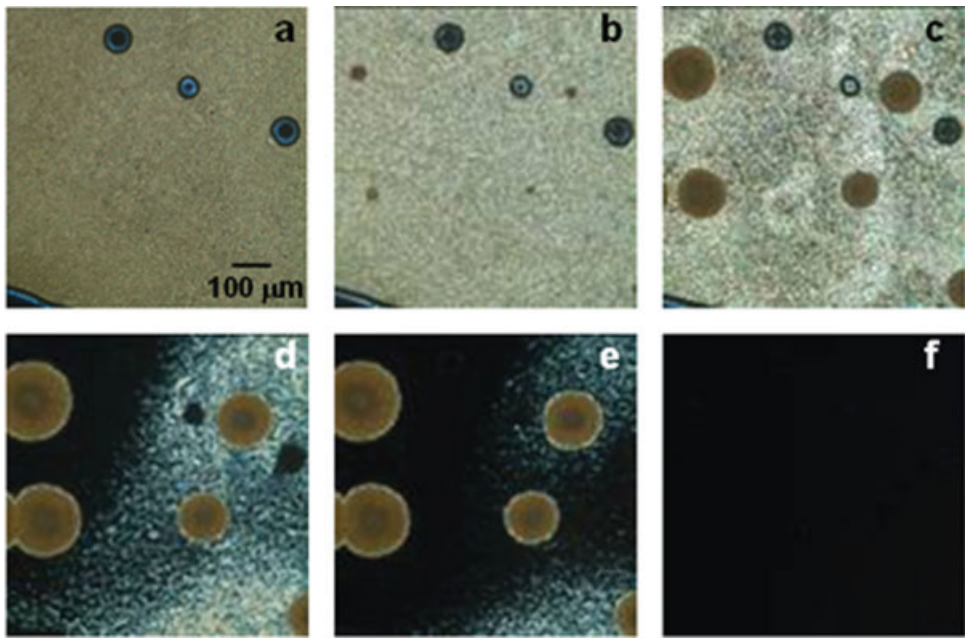

Figure 7. POM images under crossed polarizers of the $\mathbf{A^{An}1aA^{An}}$**:T1bT** 1.5:1 blend. These micrographs were acquired on the second heat at (a) 114.4 °C, (b) 144.9 °C, (c) 159.4 °C, (d) 170.3 °C, (e) 171.4 °C, (f) 201.2 °C. [Color figure can be viewed in the online issue, which is available at www.interscience.wiley.com.]

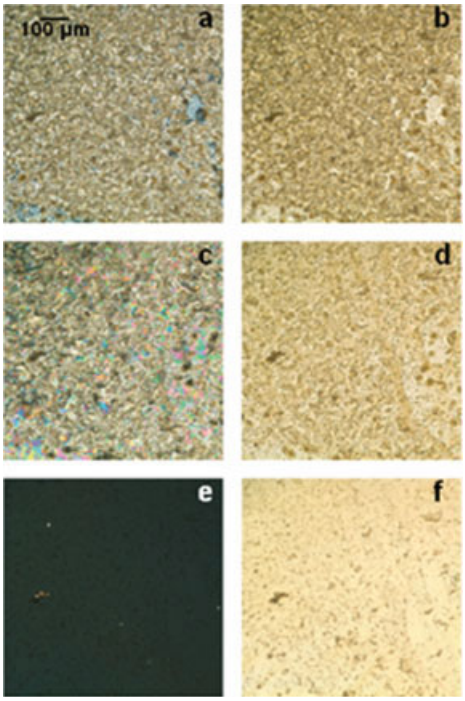

Figure 8. Comparison of the 1:1.5 $\mathbf{A^{An}1aA^{An}}$:**T1bT** blend with (a, c, and e) and without (b, d, and f) the analyzer. Data taken on heating with temperatures as follows: (a) 161.7 °C, (b) 163.1 °C, (c) 179.6 °C, (d) 180.9 °C, (e) 200.9 °C, (f) 200.8 °C.

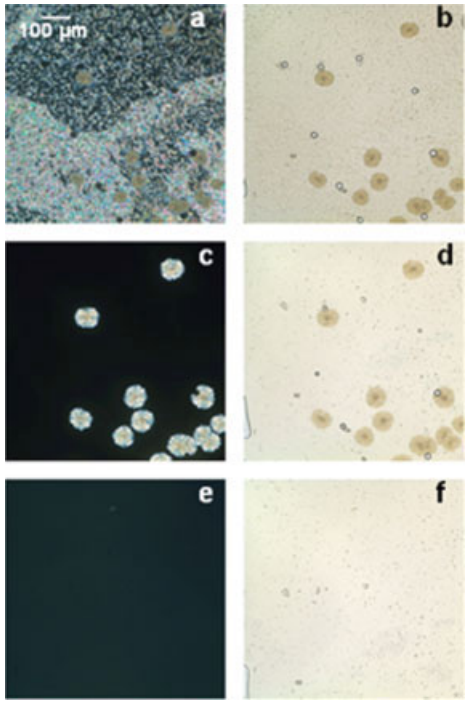

Figure 9. Comparison of the 1.5:1 $\mathbf{A^{An}1aA^{An}}$:**T1bT** blend with (a, c, and e) and without (b, d, and f) the analyzer. Data taken on heating with temperatures as follows: (a) 155.1 °C, (b) 158.1 °C, (c) 170.6 °C, (d) 172.6 °C, (e) 201.3 °C, (f) 200.9 °C.

different liquid crystalline phases: one at low temperature, but above T_g (e.g., 114 °C), and one at higher temperatures ~145 °C [Fig. 7(a,b), but lower than the crystallization exotherm that had been observed on cooling in DSC. Around 145 °C, birefringent and translucent brown spots (crystals) were observed to nucleate and grow in size with increasing temperature [Fig. 7(b–e)], despite no associated recrystallization exotherm being observed during DSC second heating. Once the blend began to transition to an isotropic phase, the crystals remained unchanged as the material around them cleared. Eventually, the crystalline spheres melted into an isotropic phase as shown in Figure 7(f). We postulate that the nucleated and grown spheres are pure $\mathbf{A^{An}1aA^{An}}$ crystals, though we cannot presently explain the absence of a calorimetric exotherm during their formation. If excess $\mathbf{A^{An}1aA^{An}}$ in such a blend spontaneously phase-separates via recrystallization, as our results suggest, a benefit to such a supramolecular system could be comparative insensitivity to blend stoichiometry that would ordinary limit polymerization degree. Thus, rheological measurements, quite sensitive to polymerization degree,

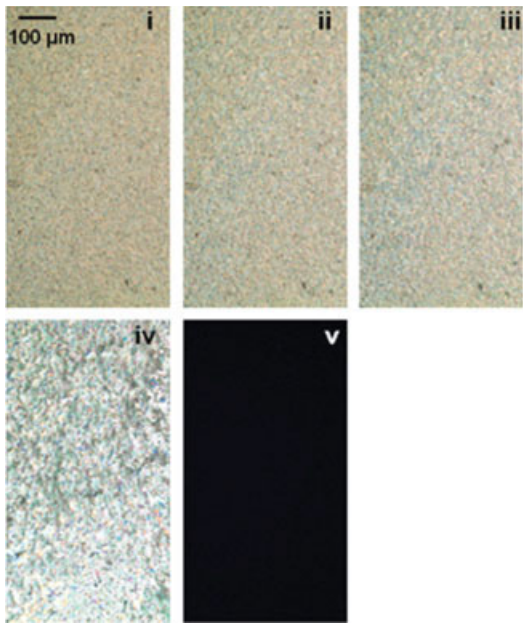

Figure 10. POM images of 1:1 $\mathbf{A^{An}1aA^{An}}$:**T1bT** blend captured on the second heat up to 230 °C at 10 °/min. Images were acquired at the following temperatures: (i) 82.4 °C, (ii) 107.0 °C, (iii) 120.0 °C, (iv) 155.4 °C, and (v) 180.0 °C.

should aid us in a future investigation of this observation of great importance to AA + BB supramolecular polymers.

To further examine the morphology of non-stoichiometric **$A^{An}1aA^{An}$:T1bT** blends, POM images were acquired at various temperatures using both crossed polarizers and with the analyzer withdrawn. For the latter optical configuration (polarized light transmitted through the sample, but with no crossed polarizer), crystalline domains are often more easily discerned from a birefringent background, appearing darker than a liquid crystalline phase because of enhanced light scattering. The micrographs from these experiments on the 1:1.5 and 1.5:1 blends of **$A^{An}1aA^{An}$:T1bT** are found in Figures 8 and 9, respectively.

Considering first the excess-**T1bT** case, the micrographs of Figure 8 reveal similar morphologies whether viewed with or without the analyzer in place, with the exception of Figure 8(c,d). These micrographs show that the recrystallized material, which was brightly colored when viewed under crossed polarizers [Fig. 8(c)], appeared to be a distinct, yet cocontinuous, phase coexisting with the liquid crystalline surrounding fluid [Fig. 8(d)]. These results are consistent with DSC results of Figure 3. Once the material appeared to lose all birefringence upon melting and viewing with the analyzer in place, removal of the analyzer revealed some remaining heterogeneity. This suggests that the material that had crystallized remained at least temporarily phase-separated from the noncrystalline fraction, possibly due to a large difference in supramolecular polymerization degree, though this is uncertain.

For comparison, examination of the excess-**$A^{An}1aA^{An}$** blend (Fig. 9) shows that the crystalline (brown) spots were present when viewed either with or without the analyzer in place. Interestingly, the spots remained stationary as the material around them melted and began to flow, indicating that these spots bridge the gap between the coverslips. After continued heating, the regions became much more clear and bright (birefringent) when viewed with the analyzer in place [Fig. 9(c)]. This suggests that these spots first melt to an LC phase, followed by isotropization, as indicated by loss of birefringence. Once the sample was fully isotropic, the spots were not present when viewed using either optical arrangement [Fig. 9(e,f)], and the isotropic phase was completely homogeneous. This proves that a single, nonbirefringent phase exists in this temperature range, as opposed to another possibility of two isotropic phases coexisting.

Finally, hot-stage POM observations of the 1:1 **$A^{An}1aA^{An}$:T1bT** were made using the same thermal protocol as for Figure 4, curves e and f; i.e., heating to a high temperature of 230 °C instead of 200 °C used in Figure 3. Thus, Figure 10 shows POM micrographs for a second heating run that followed a first heating to 230 °C. Phase transitions are indicated and consistent with the endotherms of Figure 4, curve e. Moreover, no recrystallization was observed of the type seen in Figure 5. POM micrographs observed during the subsequent cooling run from 230 °C (data not shown) nearly perfectly followed a reversal in the progression of microstructures shown in Figure 10, as expected from DSC observations. Most importantly, no evidence of recrystallization was visible, resulting in a desirable glassy liquid crystalline material. As discussed earlier, we believe that this thermal history effectively destroys high-melting crystalline nuclei that would otherwise cause crystallization in this blend.

CONCLUSIONS

In this study, we have investigated the effect that the stoichiometry of complementary nucleobase-end capped monomer units, **$A^{An}1aA^{An}$** and **T1bT**, has on the formation of supramolecular liquid crystalline phases. Although the stoichiometry appears to have little effect on the T_g of these materials, departure from the 1:1 ratio of monomers does affect the liquid crystallinity of the systems. All three samples show LC behavior; however, those systems off the 1:1 ratio exhibit more diffuse phase transitions. In addition, we have demonstrated that the behavior of these materials is very sensitive to their thermal history. The LC phases appear to be metastable and, given the appropriate thermal history (e.g., annealing for 30 min at 160 °C for the 1:1 mixture), the systems form a high melting point crystalline material, thus suppressing the liquid crystal phase. However, as the crystallization appears to be kinetically slow, heating to 230 °C (well above the melting point of the crystalline phase) allows subsequent appearance of liquid crystalline phases on cooling and on the subsequent reheating. In contrast, samples heated only to 200 °C apparently witness incomplete melting, resulting in a coexistence of crys-

talline and liquid crystalline phases. We have thus established the thermal history required for the formation of glassy liquid crystalline phases of these supramolecular materials. As such, this approach should offer a new route to intrinsically stable liquid crystal layers, coatings and devices.

This material is based upon work supported by the NIH under Grant No. NIBIB: EB-001466-01, the National Science Foundation under Grant Nos. CA-REER: CHE-0133164, CTS-0552414, a National Science Foundation Graduate Research Fellowship to KAB and by the Case School of Engineering.

REFERENCES AND NOTES

1. (a) Brunsveld, L.; Folmer, B. J. B.; Meijer, E. W.; Sijbesma, R. P. Chem Rev 2001, 101, 4071; (b) Ciferri, A. Macromol Rapid Commun 2002, 23, 511; (c) Supramolecular Polymers, 2nd ed.; Ciferri, A., Ed.; CRC Press, Taylor and Francis: Boca Raton, 2005; (d) Lehn, J.-M. Angew Chem Int Ed Engl 1990, 29, 1304.
2. For example, see: (a) Liang, Z.; Cabarcos, O. M.; Allara, D. L.; Wang, Q. Adv Mater 2004, 16, 823; (b) Kosonen, H.; Ruokolainen, J.; Knaapila, M.; Torkkeli, M.; Jokela, K.; Serimaa, R.; Brinke, G.-T.; Bras, W.; Monkman, A. P.; Ikkala, O. Macromolecules 2000, 33, 8671; (c) Tew, G. N.; Pralle, M. U.; Stupp, S. I. Angew Chem Int Ed 2000, 39, 517; (d) Percec, V.; Glodde, M.; Bera, T. K.; Miura, Y.; Shiyanovskaya, I.; Singer, K. D.; Balagurusamy, V. S. K.; Heiney, P. A.; Schnell, I.; Rapp, A.; Spiess, H.-W.; Hudson, S. D.; Duan, H. Nature 2002, 419, 384; (e) Broeren, M. A. C.; Linhardt, J. G.; Malda, H.; de Waal, B. F. M.; Versteegen, R. M.; Meijer, J. T.; Löwik, D. W. P. M.; van Hest, J. C. M.; van Genderen, M. H. P.; Meijer, E. W. J Polym Sci Part A: Polym Chem 2005, 43, 6431; (f) Lohmeijer, B. G. G.; Schubert, U. S. J Polym Sci Part A: Polym Chem 2005, 43, 6331; (g) Hawker, C. J.; Wooley, K. L. Science 2005, 309, 1200.
3. (a) Ashton, P. R.; Baxter, I.; Cantrill, S. J.; Fyfe, M. C. T.; Glink, P. T.; Stoddart, J. F.; White, A. J. P.; Williams, D. J. Angew Chem Int Ed 1998, 37, 1294; (b) Ashton, P. R.; Parsons, I. W.; Raymo, F. M.; Stoddart, J. F.; White, A. J. P.; Williams, D. J.; Wolf, R. Angew Chem Int Ed 1998, 37, 1913; (c) Yamaguchi, N.; Nagvekar, D. S.; Gibson, H. W. Angew Chem Int Ed 1998, 37, 2361; (d) Yamaguchi, N.; Gibson, H. W. Angew Chem Int Ed 1999, 38, 143; (c) Yamaguchi, N.; Gibson, H. W. Chem Commun 1999, 789; (e) Castellano, R. K.; Rudkevich, D. M.; Rebek, J., Jr. Proc Natl Acad Sci USA 1997, 94, 7132; (f) Castellano, R. K.; Nuckolls, C.; Eichhorn, S. H.; Wood, M. R.; Lovinger, A. J.; Rebek, J., Jr. Angew Chem Int Ed 1999, 38, 2603; (g) Clark, T. D.; Buriak, J. M.; Kobayashi, K.; Isler, M. P.; McRee, D. E.; Ghadiri, M. R. J Am Chem Soc 1998, 120, 8949; (h) Vollmer, M. S.; Clark, T. D.; Steinem, C.; Ghadiri, M. R. Angew Chem Int Ed 1999, 38, 1598; (i) Xu, H.; Rudkevich, D. M. Chem—Eur J 2004, 10, 5432; (j) Binder, W. H.; Kunz, M. J.; Ingolic, E. J Polym Sci Part A: Polym Chem 2004, 42, 162; (k) Kunz, M. J.; Hayn, G.; Saf, R.; Binder, W. H. J Polym Sci Part A: Polym Chem 2004, 42, 661.
4. (a) Corbin, P. S.; Zimmerman, S. C. J Am Chem Soc 1998, 120, 9710; (b) Corbin, P. S.; Zimmerman, S. C. J Am Chem Soc 2000, 122, 3779; (c) Mayer, M. F.; Nakashima, S.; Zimmerman, S. C. Org Lett 2005, 7, 3005.
5. Zeng, H.; Yang, X.; Brown, A. L.; Martinovic, S.; Smith, R. D.; Gong, B. Chem Commun 2003, 1556.
6. (a) Beijer, F. H.; Kooijman, H.; Spek, A. L.; Sijbesma, R. P.; Meijer, E. W. Angew Chem Int Ed 1998, 37, 75; (b) Beijer, F. H.; Sijbesma, R. P.; Kooijman, H.; Spek, A. L.; Meijer, E. W. J Am Chem Soc 1998, 120, 6761; (c) Söntjens, S. H. M.; Sijbesma, R. P.; van Genderen, M. H. P.; Meijer, E. W. J Am Chem Soc 2000, 122, 7487.
7. (a) Dobrawa, R.; Würthner, F. J Polym Sci Part A: Polym Chem 2005, 43, 4981; (b) Lohmeijer, B. G. G.; Schubert, U. S. J Polym Sci Part A: Polym Chem 2003, 41, 1413.
8. Sijbesma, R. P.; Beijer, F. H.; Brunsveld, L.; Folmer, B. J. B.; Hirschberg, J. H. K. K.; Lange, R. F. M.; Lowe, J. K. L.; Meijer, E. W. Science 1997, 278, 1601.
9. (a) Yang, X.; Hua, F.; Yamato, K.; Ruckenstein, E.; Gong, B.; Kim, W.; Ryu, C. Y. Angew Chem Int Ed 2004, 43, 6471; (b) Hua, F.; Yang, X.; Gong, B.; Ruckenstein, E. J Polym Sci Part A: Polym Chem 2005, 43, 1119.
10. (a) Hinderberger, D.; Schmelz, O.; Rehahn, M.; Jeschke, G. Angew Chem Int Ed 2004, 43, 4616; (b) Schmatloch, S.; van den Berg, A. M. J.; Alexeev, A. S.; Hofmeier, H.; Schubert, U. S. Macromolecules 2003, 36, 9943; (c) Dobrawa, R.; Lysetska, M.; Ballester, P.; Grüne, M.; Würthner, F. Macromolecules 2005, 38, 1315; (d) Kurth, D. G.; Meister, A.; Thuenemann, A. F.; Foerster, G. Langmuir 2003, 19, 4055; (e) Vermonden, T.; van Steenbergen, M. J.; Besseling, N. A. M.; Marcelis, A. T. M.; Hennink, W. E.; Sudhoelter, E. J. R.; Cohen Stuart, M. A. J Am Chem Soc 2004, 126, 15802; (f) Yount, W. C.; Juwarker, H.; Craig, S. L. J Am Chem Soc 2003, 125, 15302; (g) Paulusse, J. M. J.; Sijbesma, R. P. Angew Chem Int Ed 2004, 43, 4460; (h) Carlise, J. R.; Weck, M. J Polym Sci Part A: Polym Chem 2004, 42, 2973.
11. (a) Beck, J. B.; Ineman, J. M.; Rowan, S. J. Macromolecules 2005, 38, 5060; (b) Iyer, P.; Beck, J.

B.; Rowan, S. J.; Weder, C. Chem Commun 2005, 319; (c) Zhao, Y.; Beck, J. B.; Rowan, S. J.; Jamieson, A. M. Macromolecules 2004, 37, 3529; (d) Beck, J. B.; Rowan, S. J. J Am Chem Soc 2003, 125, 13922.

12. (a) Zimmerman, S. C.; Zeng, F. W.; Reichert, D. E. C.; Kolotuchin, S. V. Science 1996, 271, 1095; (b) Suárez, M.; Lehn, J.-M.; Zimmerman, S. C.; Skoulios, A.; Heinrich, B. J Am Chem Soc 1998, 120, 9526.
13. Hirschberg, J. H. K. K.; Beijer, F. H.; van Aert, H. A.; Magusin, P. C. M. M.; Sijbesma, R. P.; Meijer, E. W. Macromolecules 1999, 32, 2696.
14. Folmer, B. J. B.; Sijbesma, R. P.; Versteegen, R. M.; van der Rijt, J. A. J.; Meijer, E. W. Adv Mater 2000, 12, 874.
15. Park, T.; Zimmerman, S. C.; Nakashima, S. J Am Chem Soc 2005, 127, 6520.
16. Elkins, C. L.; Park, T.; McKee, M. G.; Long, T. E. J Polym Sci Part A: Polym Chem 2005, 43, 4618.
17. (a) Sivakova, S.; Bohnsack, D. A.; Suwanmala, P.; Mackay, M. E.; Rowan, S. J. J Am Chem Soc 2005, 127, 18202; (b) Rowan, S. J.; Suwanmala, P.; Sivakova, S. J Polym Sci Part A: Polym Chem 2003, 41, 3589.
18. (a) Sivakova, S.; Wu, J.; Campo, C. J.; Mather, P. T.; Rowan, S. J. Chem Eur—J 2006, 12, 446; (b) Sivakova, S., Rowan, S. J. Chem Commun 2003, 2428.
19. (a) Kato, T.; Fréchet, J. M. J. J Am Chem Soc 1989, 111, 8533; (b) Kato, T.; Fréchet, J. M. J. Macromol Symp 1995, 98, 311; (c) Kato, T. Supramol Sci 1996, 3, 53; (d) Kato, T.; Hirota, N.; Fujishima, A.; Fréchet, J. M. J. J Polym Sci Part A: Polym Chem 1996, 34, 57; (e) Kihara, H.; Kato, T.; Uryu, T.; Fréchet, J. M. J Chem Mater 1996, 8, 961; (f) Lee, C. M.; Griffin, A. C. Macromol Symp 1997, 117, 281; (g) Kato, T.In Handbook of Liquid Crystals, Vol. 2B; Demus, D.; Goodby, J. W.; Gray, G. W.; Spiess, H.-W.;Vill, V., Eds.; Wiley-VCH: Weinheim, 1998; p 969; (h) Kato, T. Struct Bonding 2000, 96, 95; (i) Bhowmik, P. K.; Wang, X.; Han, H. J. Polym Sci Part A: Polym Chem 2003, 41, 1282; (j) Kamikawa, Y.; Nishii, M.; Kato, T. Chem—Eur J 2004, 10, 5942; (k) Cher Ling Toh, C. L.; Xu, J.; Lu, X.; He, C. J Polym Sci Part A: Polym Chem 2005, 43, 4731.
20. (a) Lehn, J.-M. Makromol Chem Macromol Symp 1993, 69, 1; (b) Paleos, C. M.; Tsiourvas, D. Angew Chem Int Ed 1995, 34, 1696; (c) Muthukumar, M.; Ober, C. K.; Thomas, E. L. Science 1997, 277, 1225; (d) Lehn, J.-M.Supramolecular Chemistry; VCH: Weinheim, 1995; (e) Treybig, A.; Dorscheid, C.; Weissflog, W.; Kresse, H. Mol Cryst Liq Cryst 1995, 260, 369; (f) Torgova, S. I.; Strigazzi, A. Mol Cryst Liq Cryst 1999, 336, 229; (g) Percec, V.; Heck, J.; Johansson, G.; Tomazos, D.; Kawasumi, M.; Chu, P.; Ungar, G. Mol Cryst Liq Cryst Sci Technol Sect A 1994, 419, 384; (h) Percec, V. Macromol Symp 1997, 117, 267; (i) Spada, G. P; Gottarelli, G. Synlett 2004, 4, 596.
21. (a) Park, L. Y.; Hamilton, D. G.; McGehee, E. A.; McMenimen, K. A. J Am Chem Soc 2003, 125, 10586; (b) McMenimen, K. A.; Hamilton, D. G. J Am Chem Soc 2001, 123, 6453; (c) Castellano, R. K.; Clark, R.; Craig, S. L.; Nuckolls, C.; Rebek, J. Proc Natl Acad Sci USA 2000, 97, 12418; (d) Bushey, M. L.; Nguyen, T.-Q.; Zhang, W.; Horoszewski, D.; Nuckolls, C. Angew Chem Int Ed 2004, 43, 5446.
22. Hwang, I. H.; Lee, S. J.; Chang J. Y. J Polym Sci Part A: Polym Chem 2003, 41, 1881.
23. (a) Lehn J.-M. Poly Int 2002, 51, 825; (b) Kato, T.; Mizoshita, N.; Kanie, K. Macromol Rapid Commun 2001, 22, 797; (c) Paleos, C. M.; Tsiourvas, D. Liq Cryst 2001, 28, 1127; (d) Ciferri, A. Liq Cryst 1999, 26, 489.
24. (a) Gulik-Krzywicki, T.; Fouquey, C.; Lehn, J.-M. Proc Natl Acad Sci USA 1993, 90, 163; (b) Bladon, P.; Griffin, A. C. Macromolecules 1993, 26, 6604; (c) Kotera, M.; Lehn, J.-M.; Vigneron, J.-P. J Chem Soc Chem Commun 1994, 2, 197; (d) Kotera, M.; Lehn, J.-M.; Vigneron, J.-P. Tetrahedron 1995, 51, 1953; (e) St Pourcain, C.; Griffin, A. C. Macromolecules 1995, 28, 4116.